

## Identification of Markers of Taxane Sensitivity Using Proteomic and Genomic Analyses of Breast Tumors from Patients Receiving Neoadjuvant Paclitaxel and Radiation

Joshua A. Bauer<sup>1</sup>, A. Bapsi Chakravarthy<sup>2</sup>, Jennifer M. Rosenbluth<sup>1</sup>, Deming Mi<sup>3</sup>, Erin H. Seeley<sup>1</sup>, Nara De Matos Granja-Ingram<sup>4</sup>, Maria G. Olivares<sup>4</sup>, Mark C. Kelley<sup>5</sup>, Ingrid A. Mayer<sup>5</sup>, Ingrid M. Meszoely<sup>5</sup>, Julie A. Means-Powell<sup>5</sup>, Kimberly N. Johnson<sup>1</sup>, Chiaojung Jillian Tsai<sup>2</sup>, Gregory D. Ayers<sup>3</sup>, Melinda E. Sanders<sup>4</sup>, Robert J. Schneider<sup>6</sup>, Silvia C. Formenti<sup>7</sup>, Richard M. Caprioli<sup>1</sup>, and Jennifer A. Pietenpol<sup>1</sup>

### Abstract

**Purpose:** To identify molecular markers of pathologic response to neoadjuvant paclitaxel/radiation treatment, protein and gene expression profiling were done on pretreatment biopsies.

**Experimental Design:** Patients with high-risk, operable breast cancer were treated with three cycles of paclitaxel followed by concurrent paclitaxel/radiation. Tumor tissue from pretreatment biopsies was obtained from 19 of the 38 patients enrolled in the study. Protein and gene expression profiling were done on serial sections of the biopsies from patients that achieved a pathologic complete response (pCR) and compared to those with residual disease, non-pCR (NR).

**Results:** Proteomic and validation immunohistochemical analyses revealed that  $\alpha$ -defensins (DEFA) were overexpressed in tumors from patients with a pCR. Gene expression analysis revealed that MAP2, a microtubule-associated protein, had significantly higher levels of expression in patients achieving a pCR. Elevation of MAP2 in breast cancer cell lines led to increased paclitaxel sensitivity. Furthermore, expression of genes that are associated with the basal-like, triple-negative phenotype were enriched in tumors from patients with a pCR. Analysis of a larger panel of tumors from patients receiving presurgical taxane-based treatment showed that DEFA and MAP2 expression as well as histologic features of inflammation were all statistically associated with response to therapy at the time of surgery.

**Conclusion:** We show the utility of molecular profiling of pretreatment biopsies to discover markers of response. Our results suggest the potential use of immune signaling molecules such as DEFA as well as MAP2, a microtubule-associated protein, as tumor markers that associate with response to neoadjuvant taxane-based therapy. *Clin Cancer Res*; 16(2); 681–90. ©2010 AACR.

Neoadjuvant (preoperative) chemotherapy is widely used in the management of patients with locally advanced breast cancer (1–3). In addition to allowing for higher rates of breast conservation (1, 2), it permits the use of pathologic response data as an early surrogate marker for long-term clinical outcome (4, 5).

Taxanes (paclitaxel and docetaxel) are potent antimicrotubule agents and an effective treatment for breast cancer (6, 7). Although pathologic complete response (pCR) rates

for single-agent taxanes is only 5% to 15% (8–10), taxane-based combination therapy has resulted in improved pCR rates of 8% to 31%, depending on the combination (11–14). Gene expression profiling of pretreatment biopsies has generated gene signatures that can predict response to neoadjuvant combination therapies with variable accuracy (78–92%) using independent validation sets (11, 13, 14). Some signatures are as good or better than that achieved with clinical parameters alone [tumor size, nodal status, estrogen receptor (ER), progesterone receptor (PR), HER2, etc.; ref. 15]. However, use of gene signatures in the design of clinical trials or treatment has been limited. Therefore, identification of predictive markers of neoadjuvant response remains an important goal.

Several studies show taxanes as potent radiosensitizers (16–18). We and others have found that the addition of radiation to taxane-based neoadjuvant treatment increases pCR rates (30–35%) in patients with high-risk, operable breast cancer (17, 19). Despite these improved response rates, molecular markers of response to this neoadjuvant combination are not known. Thus, we used both proteomic

**Authors' Affiliations:** Departments of <sup>1</sup>Biochemistry, <sup>2</sup>Radiation Oncology, <sup>3</sup>Biostatistics, <sup>4</sup>Pathology, and <sup>5</sup>Medicine, Vanderbilt-Ingram Cancer Center, Vanderbilt University Medical Center, Nashville, Tennessee; and Departments of <sup>6</sup>Microbiology and <sup>7</sup>Radiation Oncology, New York University, New York, New York

**Note:** Supplementary data for this article are available at Clinical Cancer Research Online (<http://clincancerres.aacrjournals.org>).

**Corresponding Author:** Jennifer A. Pietenpol, Vanderbilt-Ingram Cancer Center, 652 Preston Research Building, Nashville, TN 37232. Phone: 615-936-1512; Fax: 615-936-2294; E-mail: [j.pietenpol@vanderbilt.edu](mailto:j.pietenpol@vanderbilt.edu).

doi: 10.1158/1078-0432.CCR-09-1091

©2010 American Association for Cancer Research.

and genomic technologies to analyze pretreatment biopsies with the intent of identifying markers of response to neoadjuvant paclitaxel/radiation therapy. Histology-directed matrix-assisted laser desorption/ionization mass spectrometry (MALDI-MS) allowed for the identification of differentially expressed peptides in tumor biopsies from pCR and non-pCR (NR) patients. In parallel, gene expression arrays were used to identify differentially expressed genes.

## Materials and Methods

**Patients and neoadjuvant treatment.** Women with high-risk (stages IIA-IIIIB), operable breast cancer were treated with three cycles of paclitaxel (175 mg/m<sup>2</sup> every 3 wk), followed by twice weekly paclitaxel (30 mg/m<sup>2</sup>) and concurrent radiation. Patients underwent definitive surgery after completion of chemoradiation (19). Tissue samples were taken from individuals treated at Vanderbilt University or New York University Medical Centers with institutional review board approval. All patients signed a protocol-specific consent. Pretreatment core biopsies were analyzed for ER, PR, and HER2 as previously described and scored by a breast pathologist (19). HER2 amplification was confirmed by fluorescence *in situ* hybridization when immunohistochemistry score was 2+. pCR was defined as the absence of any invasive cancer and NR was defined as any viable tumor in breast or lymph nodes (partial response) or those with progressive disease. pCR and NR were determined from the primary pathologic slide at the time of surgery by a breast pathologist. Median follow-up time for surviving patients was 51 mo (range, 40-73 mo).

**Histology-directed MALDI-MS and proteomic data analysis.** For MALDI-MS profiling, serial sections from each frozen biopsy were H&E-stained or thaw-mounted and fixed onto a MALDI plate. Photomicrographs of H&E-stained sections were annotated to mark areas (~200 μm, minimum of 10 spots) of interest for both tumor and stroma by a breast pathologist for matrix spotting. All normal, dysplastic or necrotic tissue, areas of inflammation, potential contamination (e.g., blood), and edges of tumor sections were avoided. Annotated H&E images were overlaid with MALDI plate images to extract coordinates for robotic spotting. An acoustic robotic spotter (LabCyte) placed crystalline matrix (20 mg/mL sinapinic acid in 1:1 acetonitrile/0.2% trifluoroacetic acid) spots (180-220 μm in diameter) on each tissue. Tissue profile spectra were acquired using an Autoflex II (Bruker Daltonics) MALDI mass spectrometer and run using an automated linear mode acquisition method optimized for 2 to 40 kDa peptides, as previously described (20). Experiments were repeated on separate dates to account for experimental variation. MALDI-MS spectra were baseline corrected, normalized, and aligned using ProTS-Marker (Biosesix). Multiple spectra ( $n \geq 10$ ) were averaged from the same subject from different experiments for tumor and stroma. Peak intensities of 115 candidate features from processed spectra were log-transformed from the 13 NR and 6 pCR biopsies.

Significance analysis of microarrays and linear mixed effects model (for intrasubject and intersubject variability) were used to identify differential features between NR and pCR samples. A permutation test ( $n = 10,000$ ) was used to determine the significance ( $<0.05$ ) by controlling for the false discovery rate (FDR).  $P$  values (significance  $< 0.05$ ) from linear mixed effects model were not adjusted for multiple testing. Differential features of interest were identified using both methods.

MALDI-MS imaging experiments were done by coating the tissue surface with matrix, spectra were acquired at each position on the sample at a spatial resolution of 100 μm, and spectral files were reconstructed into ion density images for viewing.

**Immunohistochemistry.** Immunohistochemistry on tissue sections were processed as previously described (21). Briefly, paraffin-embedded breast tissue sections were mounted and deparaffinized in xylene. Antigen retrieval was achieved by microwaving slides in 10 mmol/L of citrate buffer (pH 6.0). Slides were permeabilized in a 1:1 acetone/methanol solution, washed, and incubated in 3% hydrogen peroxide. Blocking was continued using Dako Protein Block (Dako). Sections were incubated with  $\alpha$ -defensin (DEFA) antibody (AbD Serotec) diluted 1:1,000 for 1 h at 25°C followed by exposure to a labeled streptavidin-biotin system (Dako). Scoring for immunohistochemical staining of DEFA and MAP2 and inflammation are described in the Supplementary Materials and Methods.

**Gene expression profiling and data analysis.** Of the 38 patients, 14 had sufficient tissue (4 with pCR, 10 with NR) for quality RNA. Invasive tumor cells from serial sections were captured onto polymeric caps using the PixCell II laser capture microdissection system (Arcturus). Areas of ductal carcinoma *in situ* and normal breast tissue were excluded and areas of inflammation were avoided. Total RNA was isolated from captured cells, quantified, integrity analyzed, and microarray analyses done as previously described using Affymetrix GeneChip Human Genome U133 Plus 2.0 arrays (Affymetrix; ref. 22). Data from duplicate RNA samples from each biopsy ( $n = 28$ ) were imported into GeneSpring GX (version 10.0.2) software (Agilent). Probe level analysis was done using Guanine Cytosine Robust Multi-Array analysis that includes background correction, quantile normalization, and probe summarization. Probe sets were log-transformed and averaged among duplicate samples. An unpaired  $t$  test was used to identify differential expression of genes between pCR and NR samples. A FDR multiple testing  $t$  test (Benjamini-Hochberg) was used to generate corrected  $P$  values for each probe (23). A heat map was generated to show differentially expressed probes. An enrichment-based statistical test was used to generate  $P$  values for gene ontology categories using GeneSpring.

**Cell culture and cell engineering.** MCF-7 and MDA-MB-468 cells were cultured in DMEM supplemented with 10% fetal bovine serum, 10 μg/mL insulin (MCF-7 cells), and 1% penicillin-streptomycin as previously described (24). All cells were cultured at 37°C with 5% CO<sub>2</sub>. For three-dimensional culture models, cells were seeded on growth

factor-reduced Matrigel (BD Biosciences) as previously described (25–27). Paclitaxel (Sigma-Aldrich) was added 24 h after cell seeding and replaced every 3 d. Mammospheres were digested, trypsinized, and single cells counted using a hemocytometer.

To generate stable cell lines, MAP2 cDNA was cloned into the FG12 lentiviral vector. Viral production and gene transduction were done as previously described (28).

**Immunoblotting.** Cell lysates were immunoblotted as previously described using a MAP2 antibody, dilution 1:500 (Lab Vision/NeoMarkers), and a GAPDH antibody at a dilution of 1:1,000 (Chemicon International; ref. 21).

**Biomarker analysis and taxane-neoadjuvant patients.** For biomarker analysis, 64 pretreatment biopsies were obtained from patients that received taxane-based neoadjuvant chemotherapy. Patients were classified into those that received taxane-based neoadjuvant treatments including (a) paclitaxel/radiation, (b) dose-dense docetaxel alone, or (c) Adriamycin/cyclophosphamide followed by paclitaxel. Clinical variables (e.g., age, ER/PR, etc.) for patient and treatment comparisons are shown in Supplementary Table S1. Weighted index of MAP2 expression by immunohistochemical scoring was summarized using the median and interquartile range (25th to 75th percentile). Linear pair-wise correlations among variables were estimated using Spearman's correlation. The odds of a pCR for a unit change in DEFA expression or inflammation and an interquartile change in MAP2 expression were

estimated using logistic regression.  $P < 0.05$  was considered statistically significant.

## Results

**Neoadjuvant paclitaxel/radiation.** Patients with high-risk, operable breast cancer were treated with three cycles of paclitaxel followed by concurrent paclitaxel/radiation. Previously, we reported that mitotic index was a significant prognostic marker of response (pCR = 34%) to this presurgical therapy (19). For this study, we obtained sufficient tumor tissue from the same patient cohort to perform proteomic and gene expression analyses on 19 and 14 patients, respectively (Table 1).

**Proteomic tumor profiling.** We performed histology-directed MALDI-MS to identify protein markers of response to neoadjuvant paclitaxel/radiation from 19 of the 38 patients (6 with pCR) for which sufficient tissue was available. This technique allows for cellular specificity (200  $\mu\text{m}$  diameter) and the generation of protein profiles for biomarker discovery (20). MALDI-MS profiles from each annotated tumor and stroma area were collected and averaged for each biopsy. Average tumor spectra from the 6 pCR and 13 NR patients were compared using two statistical methods (see Materials and Methods) to identify differentially expressed features (i.e., peak intensity of each  $m/z$ ). Average NR spectra intensity was offset ( $y = +400$ ) to visually compare differences in average pCR spectra (Fig. 1). Three features

**Table 1. Patient profiles and tumor features**

Patient no.	ER	PR	HER2*	pCR	Outcome	Analyses	
						Proteomics	Microarray
1	+	+	–	No	AWD	Yes	Yes
2	+	–	–	No	NED	Yes	Yes
3	+	+	+	No	NED	Yes	Yes
4	+	+	–	No	NED	Yes	Yes
5	–	–	–	No	AWD	Yes	Yes
6	–	–	–	No	AWD	Yes	Yes
7	–	–	+	No	DOD	Yes	No
8	+	–	–	No	DOD	Yes	Yes
9	–	–	+	No	DOD	Yes	Yes
10	+	+	–	No	DOD	Yes	Yes
11	–	–	+	No	DOD	Yes	No
12	–	–	–	No	DOD	Yes	No
13	–	–	+	No	DOD	Yes	Yes
14	–	–	+	Yes	NED	Yes	No
15	–	–	–	Yes	NED	Yes	Yes
16	–	–	–	Yes	NED	Yes	Yes
17	–	–	–	Yes	NED	Yes	No
18	–	–	–	Yes	NED	Yes	Yes
19	–	–	–	Yes	NED	Yes	Yes

Abbreviations: DOD, dead of disease; NED, no evidence of disease; AWD, alive with disease.

\*HER2+ determined both by immunohistochemistry ( $\geq 2+$ ) and fluorescence *in situ* hybridization ( $>2$  copies).

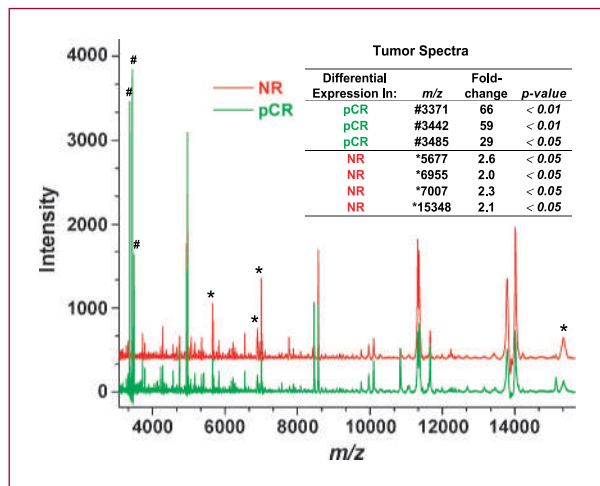


**Fig. 1.** Average tumor spectra of pCR (green) and NR (red) from MALDI-MS. Inset, the differentially expressed *m/z* peaks that were higher (#) or lower (\*) in pCR versus NR. Fold change was calculated using significance analysis of microarrays. *P* values were generated using the linear mixed effects model.

(*m/z* = 3371, 3442, and 3485) were overexpressed >30-fold ( $P < 0.05$ ) and four features (*m/z* = 5677, 6955, 7007, and 15348) were underexpressed >2-fold ( $P < 0.05$ ) in patients with pCR. No statistically significant, differentially expressed features were observed in the stroma profiles ( $n = 19$ ) of pCR and NR biopsies (data not shown).

The three most significant peaks, *m/z* = 3371, 3442, and 3485 (Fig. 2A), have previously been identified as  $\alpha$ -DEFA1,  $\alpha$ -DEFA2, and  $\alpha$ -DEFA3, respectively (29–31). DEFA3 is a family of microbicidal and cytotoxic peptides involved in phagocyte-mediated host defense and are abundant in neutrophil granules (32). To eliminate the possibility that DEFA peptides were present as an artifact of contaminating blood in the biopsy material (33), we first evaluated the tumor specimens for the presence of histone H4 peptides, which are abundant in nucleated cells (Fig. 1; peaks *m/z* = 11,307 and 11,349). More significantly, our tumor MALDI spectra lacked hemoglobin peaks (*m/z* = 7,564 and 7,835 or 15,127 and 15,668; Fig. 1), which are highly abundant in blood-contaminated specimens (33).

To validate our proteomic profiling-based findings and to identify the source of DEFA expression, we analyzed pre-treatment biopsies by immunohistochemistry with a DEFA-specific antibody. Several patients who achieved pCRs (nos. 14 and 19) showed robust DEFA expression in tumor cells and tumor stromal areas, whereas there was little to no DEFA expression in NR tumors (nos. 9 and 11; Fig. 2B). Of note, infiltrating neutrophils stained positive for DEFA expression in all sections indicating the specificity of the antibody.

To further ensure that there was no bias to detect DEFA expression based on placement of matrix spots, MALDI-MS imaging was done on the entire tissue section to allow visualization of the spatial distribution of DEFA across a biopsy section. One representative NR and pCR sample showed that DEFA1 and DEFA2 were present in both tu-

mor and stroma of patients who achieved a pCR, but was absent in patients that did not (NR; Fig. 2C). Of note, DEFA peptides were only identified in areas of tumor (compare H&E and MALDI-MS images in Fig. 2C), suggesting that DEFA are specifically expressed in tumor cells or surrounding stroma and not just present due to whole blood contamination. Nonetheless, any future consideration of DEFA as a biomarker would need to take into account the use of tissue that is not contaminated with tumor-associated blood as we have done in this study. Also, we cannot rule out the possible contribution of neutrophils to DEFA expression in areas of tumors with high levels of neutrophil infiltrate. Consistent with our results, DEFA expression has been shown to be prevalent in squamous cell carcinomas (30). These profiling and imaging data show for the first time that histology-directed MALDI-MS could accurately identify differential features in pre-treatment biopsies that correlate with response and show the use of proteomics for future biomarker analyses.

**Gene expression profiling.** Gene expression profiling was used to identify differential expression patterns that correlated with response to neoadjuvant paclitaxel/radiation treatment in 14 patients (4 with pCR). Laser capture microdissection was done because there was significant heterogeneity in the biopsies with tumor cellularity ranging from 20% to 95%. RNA isolated from captured tumor cells was hybridized to Affymetrix GeneChips. We first annotated pCR and NR gene expression data and did an unpaired *t* test on all probes to identify differentially expressed genes. A heat map was generated for a 101-probe set that represents genes with a >3-fold change in expression ( $P < 0.05$ ) between pCR and NR samples (Fig. 3A). MAP2, microtubule-associated protein 2, which had a >4-fold change in expression as assessed by two probes was a highly significant, differentially expressed gene (FDR-corrected *t* test,  $P < 0.03$ ) in tumors from patients with pCR versus NR (Fig. 3B).

Because MAP2 binds and stabilizes microtubules, and paclitaxel treatment enhances this interaction, which may contribute to drug sensitivity, we chose to further study this gene as a marker of paclitaxel sensitivity (34). MAP2 overexpression has been observed in several types of cancers (35–39). We obtained basal MAP2 mRNA expression from five breast cancer cell lines and the concentration of paclitaxel at which their growth was inhibited by 50% ( $GI_{50}$  values; see Supplementary Materials and Methods). The expression of MAP2 in the breast cancer cell lines is highly correlated ( $R^2 > 0.99$ ) with paclitaxel sensitivity *in vitro* (Supplementary Fig. S1). These data suggest that MAP2 expression is a critical determinant of taxane sensitivity in breast cancers.

To determine if a mechanistic link exists between levels of MAP2 protein and taxane sensitivity, we engineered two breast cancer cell lines, MCF-7 and MDA-MB-468, to overexpress MAP2. Both cell lines were transduced with a vector containing MAP2 cDNA or empty vector. Stable overexpression of MAP2 was confirmed in MCF-7 and MDA-MB-468 cells by immunoblot analysis (Fig. 4A). The cells were

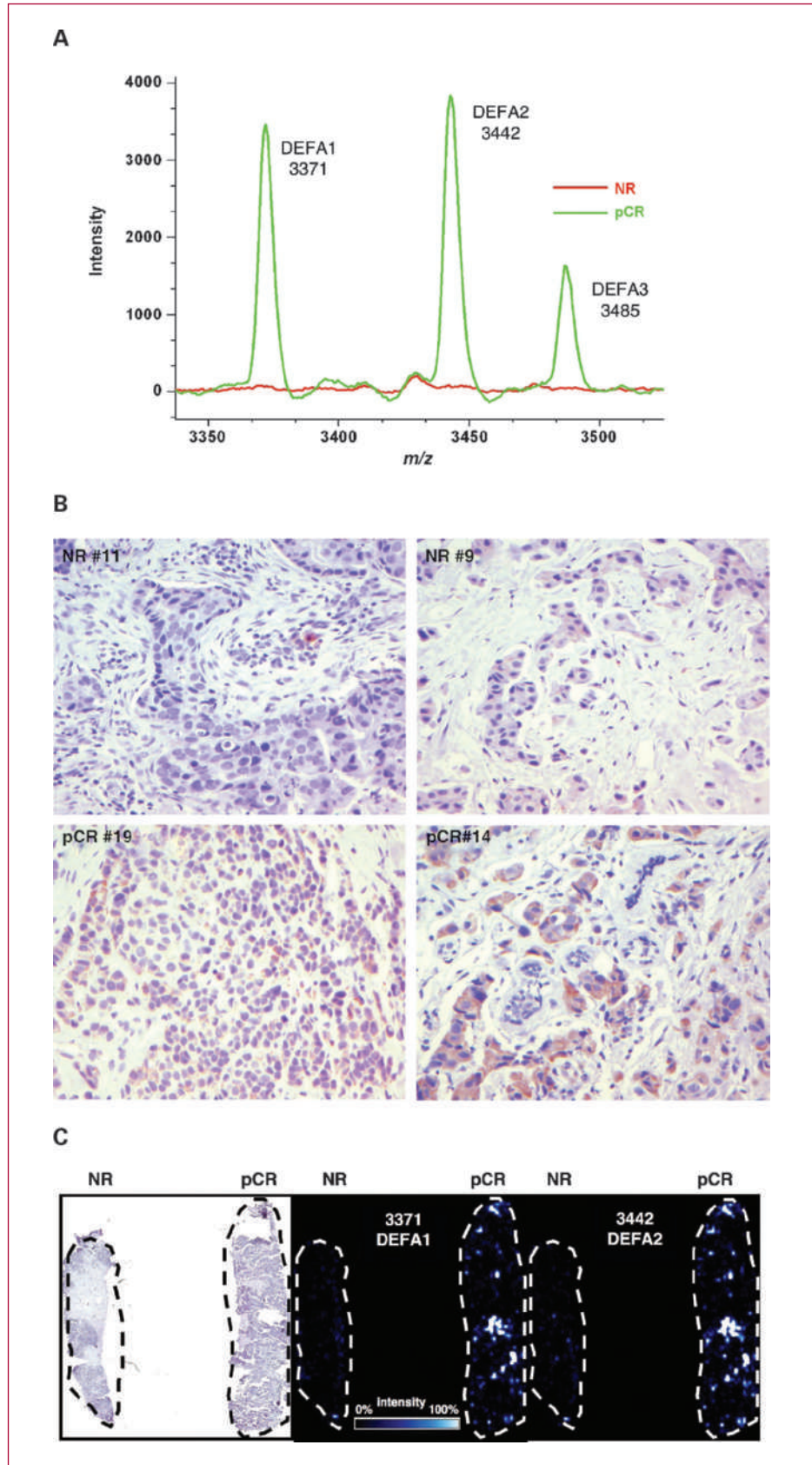


**Fig. 2.** A, average pCR (green) and NR (red) spectra peaks for DEFA1-3. B, immunohistochemical analysis for DEFAs from two representative pCR and NR tumors. C, MALDI-MS imaging of DEFA1 and DEFA2 was done by overlaying spectral files that were reconstructed into ion density images with an H&E image (left) of an NR and pCR for visualization.

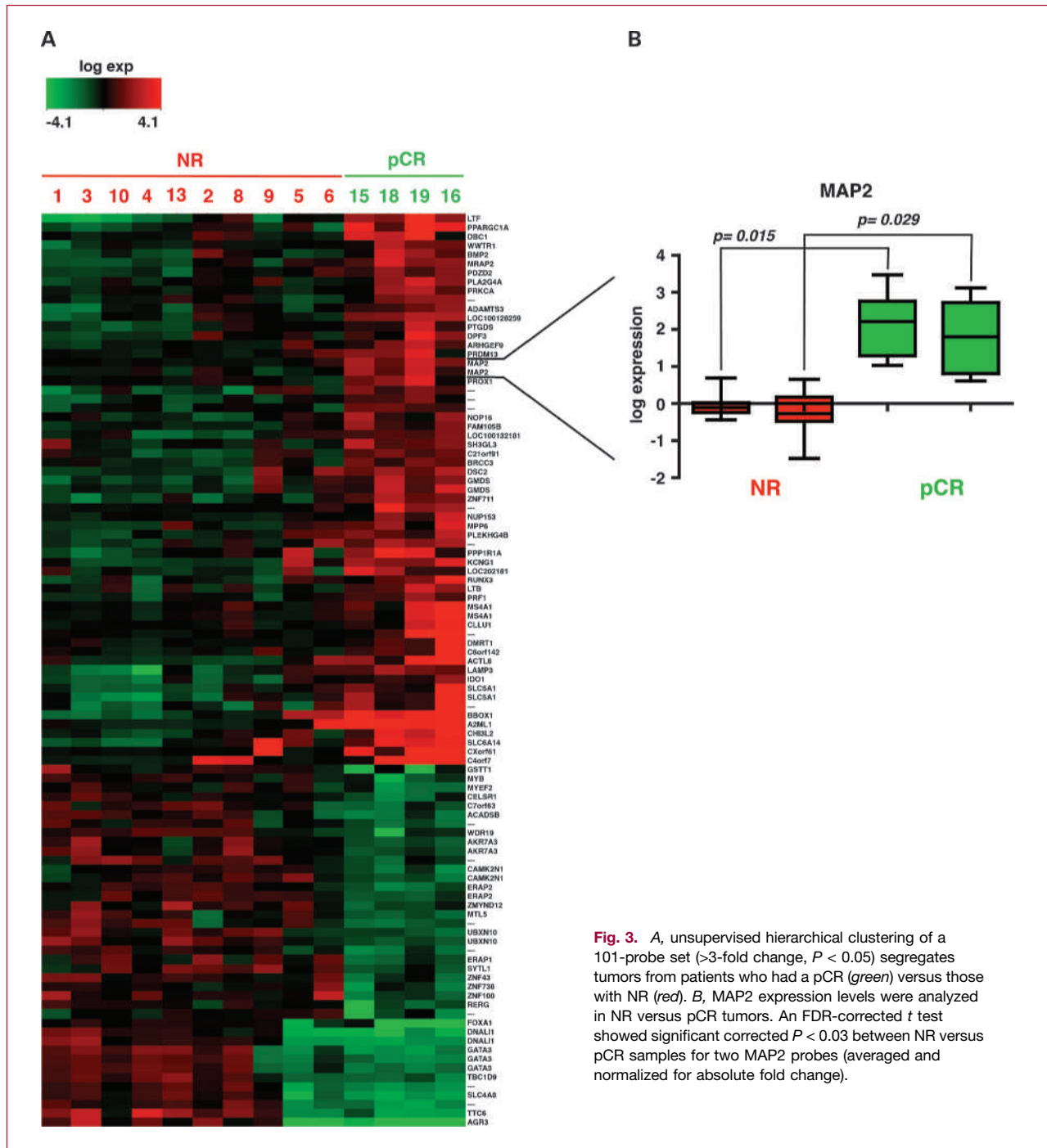


**Fig. 3.** A, unsupervised hierarchical clustering of a 101-probe set (>3-fold change,  $P < 0.05$ ) segregates tumors from patients who had a pCR (green) versus those with NR (red). B, MAP2 expression levels were analyzed in NR versus pCR tumors. An FDR-corrected  $t$  test showed significant corrected  $P < 0.03$  between NR versus pCR samples for two MAP2 probes (averaged and normalized for absolute fold change).

Downloaded from <http://aacrjournals.org/clincancerres/article-pdf/16/2/681/1993304/681.pdf> by guest on 08 October 2024

grown as three-dimensional mammospheres, a culture method that has been well characterized and recapitulates breast epithelial function and morphology (25–27). Paclitaxel treatment reduced mammosphere formation and overall cell number by 53.7% and 46.4% in MCF-7 and MDA-MB-468 cells overexpressing MAP2 relative to vector control, respectively (Fig. 4B). We also examined the sensitivity of these engineered breast cancer cell lines to paclitax-

el when grown as two-dimensional colonies and observed a similar phenomenon (data not shown).

Having identified individual biomarkers that influence response to paclitaxel, we used our gene expression data to explore clinical subgroups of tumors associated with response. Gene expression profiling has resulted in the molecular classification of breast cancers into five distinct subtypes: normal breast, HER2+, basal-like, luminal-A,

and luminal-B (40–42). The basal-like subtype is predominantly composed of triple-negative breast cancers (43, 44). Cross-referencing the gene signature that defines these molecular subtypes to our set of probes that had >3-fold change in expression in pCR versus NR ( $P < 0.05$ ) resulted in subtype classification of these tumors. For example, we observed the overexpression of 9 of 19 (*ACTG2*, *SLPI*,

*ANXA8*, *KRT5*, *TRIM29*, *KRT17*, *GAPRP*, *FOXC1*, and *CH13L2*) known genes in the basal-like signature and the downregulation of 5 of 13 genes (*TFF3*, *ESR1*, *GATA3*, *ACADSB*, and *REGG*) in the luminal signature as previously defined (43), in patients that experienced a pCR (Supplementary Table S2). Similarly, expression of ER-regulated genes (e.g., *GATA3* and *REGG*) was found in ER+ patients

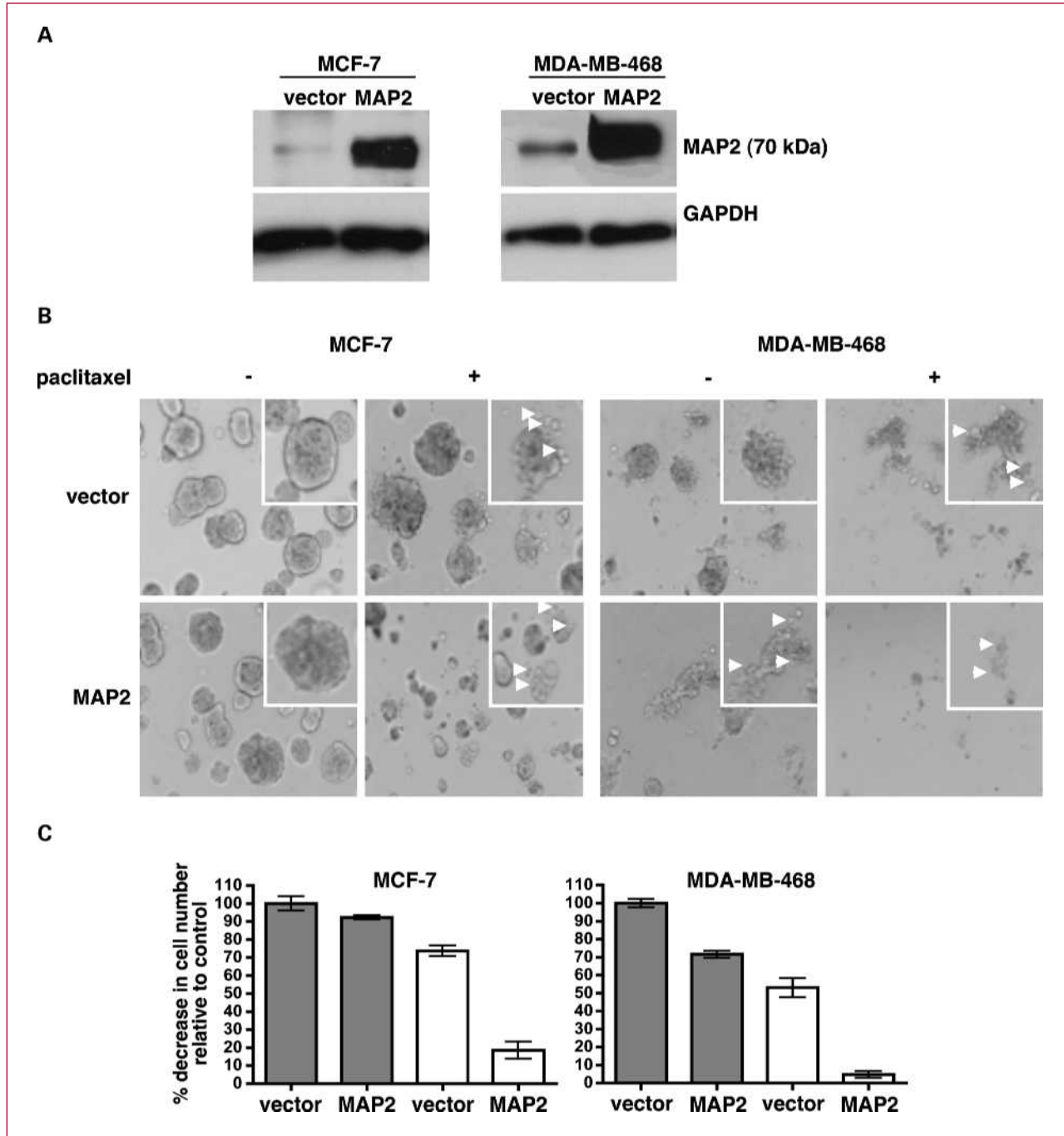


**Fig. 4.** A, Western analyses showing MAP2 and GAPDH protein levels in MCF-7 and MDA-MB-468 cells transduced with vector control or MAP2. B, control and MAP2-expressing cells were grown as mammospheres ± paclitaxel. Arrows, nonadherent or apoptotic cells. The number of viable cells was determined after 10 d ± paclitaxel and represented relative to untreated control.

that lacked a response (NR). These observations are also in concordance with our finding that five of six patients with a pCR had triple-negative tumors (Table 1). Of note, the number of triple-negative tumors molecularly analyzed herein was similarly proportioned to those enrolled overall in the study, eliminating potential sampling bias.

An enrichment-based statistical test was used for gene ontology categories for probes that were differentially expressed between patients with pCR versus NR (>3-fold;  $P < 0.05$ ). There was a significant enrichment for immune signaling categories, including defense response, immune response, MHC complexes, response to stimulus, chemokine activity, and immune cell activation (Supplementary Table S3).

**Biomarker validation in another patient cohort receiving taxane-based neoadjuvant treatment.** To further validate if the expression of the two markers, DEFA and MAP2, was associated with pCR in an independent patient cohort, we obtained tissue from 47 additional pretreatment biopsies from patients treated with neoadjuvant taxane-based chemotherapy and evaluated DEFA and MAP2 expression by immunohistochemistry (Supplementary Table S1). Eleven of 47 (23%) of the patients in the second cohort which received taxane-based neoadjuvant therapy achieved a pCR. In addition, because DEFA is a marker of neutrophils and our gene expression and gene ontology analyses of tumors from patients with pCR revealed a link to host immune response, we also scored the biopsy specimens for immune cell infiltrate surrounding the tumor as a marker of inflammation as well as counted neutrophils within the infiltrate (as described in Materials and Methods). We found that six tumors (9% of total) had high levels of neutrophil infiltrate (>10/high-power field) of which three tumors were from patients that achieved a pCR (Supplementary Fig. S2B; data not shown).

Univariate logistic regression of pCR indicated statistically significant associations with all three markers, DEFA ( $P = 0.007$ ), inflammation ( $P = 0.031$ ), and MAP2 ( $P =$

0.037) as assessed by immunohistochemistry. Increases in DEFA expression and levels of inflammation were associated with an increase in the odds of achieving a pCR of 3.4 (95% confidence interval, 1.4-8.1) and 2.3 (95% confidence interval, 1.1-4.9), respectively (Table 2). Of note, DEFA, a neutrophil marker, had correlation with inflammation in tumor samples ( $r = 0.36$ ,  $P = 0.007$ , Spearman's correlation). pCR was 3.2 times (95% confidence interval, 1.1-9.3) more likely in a patient with MAP2 at the 75th percentile than a patient at the 25th percentile (Table 2). Statistical significance was not reached in a multivariable analysis of all three markers (data not shown), likely due to the limited number of pCRs in this patient cohort. Definitive multivariate evaluation of these markers is warranted in larger patient cohorts that have received neoadjuvant taxane-based therapy.

## Discussion

We used proteomic and genomic analyses to identify molecular markers of pCR to neoadjuvant paclitaxel/radiation treatment. A marker of inflammation, DEFA, higher levels of tumor-infiltrating immune cells, and a microtubule-associated protein 2 (MAP2), were all found to be differentially expressed between pCR and NR tumor biopsies. To validate our findings, we showed that these markers were significantly associated with response in a separate cohort of patients receiving taxane-based neoadjuvant therapy.

Of the 38 patients enrolled in our study, 12 were triple-negative and of those 58% (7 patients) had a pCR. Only 23% of patients with non-triple-negative tumors achieved pCR. Thus, patients with triple-negative disease are twice as likely to respond to this treatment regimen. Likewise, in two independent studies, the basal-like (triple negative) and HER2+ subgroups were found to be associated with higher rates of pCR (27-45%), versus luminal pCR rates (6-7%), in patients receiving taxane-based neoadjuvant treatment (45, 46). Of note, with further follow-up, patients that achieved

**Table 2. Biomarker analysis in taxane-neoadjuvant breast cancer biopsies**

	Score	NR, n (% of score)	pCR, n (% of score)	OR (95% CI)
DEFA	0	8 (100%)	0 (0%)	3.4 (1.4-8.1), $P = 0.007$
	+1	17 (81.0%)	4 (19.1%)	
	+2	13 (56.5%)	10 (43.5%)	
	+3	2 (40.0%)	3 (60.0%)	
Inflammation	0	4 (100%)	0 (0%)	2.3 (1.1-4.9), $P = 0.031$
	+1	22 (88.0%)	3 (12.0%)	
	+2	13 (61.9%)	8 (38.1%)	
	+3	7 (63.6%)	4 (36.4%)	
MAP2*		P50 (P25-P75)	P50 (P25-P75)	3.2 (1.1-9.3), $P = 0.037$
		33.3 (18.3-38.3)	35.0 (31.7-40.0)	

Abbreviations: P50, median (P25, 25th percentile; P75, 75th percentile); OR, odds ratio; 95% CI, 95% confidence interval.

\*Weighted index of MAP2 expression (Materials and Methods).



a pCR have remained disease-free (median follow-up of 59 months) to date, indicating the importance of identifying molecular markers of response.

Proteomic analysis identified DEFAs as predictors of pCR. DEFAs play an important role in innate immune defense against inflammatory-related diseases, including epithelial tumors (30, 47). DEFA expression was also associated with high levels of inflammation and immune cell infiltrate. Furthermore, from gene expression profiling and statistical testing to analyze differentially expressed genes between pCR versus NR patients, we observed a significant enrichment for immune response categories. Of note, DEFAs were not differentially expressed by gene profiling, likely because DEFAs are regulated at the posttranslational level of granule processing (32).

Using gene expression profiling, a recent study of triple-negative tumors found that tumors with increased lymphocytic infiltrate and high expression of IFN-regulated and immunoglobulin genes are associated with improved metastasis-free survival (44). The IFN-regulated gene (*CXCL10*) and two immunoglobulin genes (*IGHG1* and *IGHG3*) that cluster with triple-negative tumors in the study were found to be increased (>3-fold) in tumors from patients with pCR (data not shown). These data suggest that expression of immunologically related proteins, such as DEFAs, and the presence of immune cell infiltrate in triple-negative breast tumors might be predictive of response to neoadjuvant paclitaxel/radiation treatment, and that additional molecular insights could be gained from the integrated use of both genomic and proteomic tumor profiling.

From our microarray analysis, we found that *MAP2* was expressed at a higher level in pCR versus NR tumors ( $P < 0.03$ ). *MAP2* plays a critical role in neurite outgrowth and dendrite development through its microtubule-stabilizing function (48), and is expressed in non-small cell (38), neuroendocrine (35, 37), and oral squamous cell carcinomas (36). Expression of *MAP2* in metastatic melanoma cells leads to microtubule stabilization, G<sub>2</sub>-M cell cycle arrest, and growth inhibition *in vitro* and *in vivo* (39). Primary melanomas with high *MAP2* expression have significantly better metastatic disease-free survival than those with little or no expression. *MAP2*-related peptides are highly expressed in docetaxel-sensitive pancreatic ductal adenocarcinoma compared with docetaxel-refractory pancreatic cancers (49). Paclitaxel treatment enhances the interaction between

tubulin and *MAP2*, which may contribute to taxane sensitization in cells with high *MAP2* expression (34). Supporting this theory, we found that *MAP2* overexpression in two breast cancer cell lines correlated with paclitaxel sensitivity. Pretreatment expression of *MAP2* in breast tumor biopsies may serve as a marker of response to taxane-based neoadjuvant treatment.

Taxane treatment remains one of the most effective therapies for breast cancer in the neoadjuvant, adjuvant, and metastatic settings as well as improving both disease-free and overall survival (8, 50). DEFA and *MAP2* expression and immune infiltration were significantly associated with pCR in a large spectrum of patients that received neoadjuvant taxane-based therapy. These biomarkers may have future utility for the selection of breast cancer patients that receive taxanes as part of their treatment regimen.

### Disclosure of Potential Conflicts of Interest

A.B. Chakravarthy: commercial research grants for the support of the clinical trials from Aventis and BMS. The other authors disclosed no potential conflicts of interest.

### Acknowledgments

We thank the participating patients, the research nurses who assisted with sample collection, Rakesh Reddy and Theresa Adkins for clinical data entry, and Carlos Arteaga for insight and review of the manuscript.

### Grant Support

NIH grants P50 CA95131 (Specialized Program of Research Excellence in Breast Cancer); CA105436 and CA070856 (J.A. Pietenpol); ES00267 and CA68485 (core services); CA009385 (J.A. Bauer); 5R01 GM58008-09 (R.M. Caprioli); Department of Defense W81XWH-05-1-0179 (R.M. Caprioli); U.S. Army grant DAMD17-99-1-9422 (J.A. Pietenpol); and a Vanderbilt-Ingram Cancer Center Discovery Grant (A.B. Chakravarthy).

The costs of publication of this article were defrayed in part by the payment of page charges. This article must therefore be hereby marked *advertisement* in accordance with 18 U.S.C. Section 1734 solely to indicate this fact.

Received 5/4/09; revised 9/30/09; accepted 10/25/09; published OnlineFirst 1/12/10.

### References

- Bear HD, Anderson S, Brown A, et al. The effect on tumor response of adding sequential preoperative docetaxel to preoperative doxorubicin and cyclophosphamide: preliminary results from National Surgical Adjuvant Breast and Bowel Project Protocol B-27. *J Clin Oncol* 2003;21:4165-74.
- Fisher B, Bryant J, Wolmark N, et al. Effect of preoperative chemotherapy on the outcome of women with operable breast cancer. *J Clin Oncol* 1998;16:2672-85.
- Kaufmann M, von Minckwitz G, Smith R, et al. International expert panel on the use of primary (preoperative) systemic treatment of operable breast cancer: review and recommendations. *J Clin Oncol* 2003;21:2600-8.
- Chollet P, Amat S, Cure H, et al. Prognostic significance of a complete pathological response after induction chemotherapy in operable breast cancer. *Br J Cancer* 2002;86:1041-6.
- Kuerer HM, Newman LA, Smith TL, et al. Clinical course of breast cancer patients with complete pathologic primary tumor and axillary lymph node response to doxorubicin-based neoadjuvant chemotherapy. *J Clin Oncol* 1999;17:460-9.
- Hortobagyi G. Docetaxel in breast cancer and a rationale for combination therapy. *Oncology (Huntingt)* 1997;11:11-5.
- Hortobagyi GN. Paclitaxel-based combination chemotherapy for breast cancer. *Oncology (Huntingt)* 1997;11:29-37.
- Buzdar AU, Singletary SE, Theriault RL, et al. Prospective evaluation

- of paclitaxel versus combination chemotherapy with fluorouracil, doxorubicin, and cyclophosphamide as neoadjuvant therapy in patients with operable breast cancer. *J Clin Oncol* 1999;17:3412–7.
9. Chan S, Friedrichs K, Noel D, et al. Prospective randomized trial of docetaxel versus doxorubicin in patients with metastatic breast cancer. *J Clin Oncol* 1999;17:2341–54.
  10. Sledge GW, Neuberg D, Bernardo P, et al. Phase III trial of doxorubicin, paclitaxel, and the combination of doxorubicin and paclitaxel as front-line chemotherapy for metastatic breast cancer: an intergroup trial (E1193). *J Clin Oncol* 2003;21:588–92.
  11. Ayers M, Symmans WF, Stec J, et al. Gene expression profiles predict complete pathologic response to neoadjuvant paclitaxel and fluorouracil, doxorubicin, and cyclophosphamide chemotherapy in breast cancer. *J Clin Oncol* 2004;22:2284–93.
  12. Dressman HK, Hans C, Bild A, et al. Gene expression profiles of multiple breast cancer phenotypes and response to neoadjuvant chemotherapy. *Clin Cancer Res* 2006;12:819–26.
  13. Hess KR, Anderson K, Symmans WF, et al. Pharmacogenomic predictor of sensitivity to preoperative chemotherapy with paclitaxel and fluorouracil, doxorubicin, and cyclophosphamide in breast cancer. *J Clin Oncol* 2006;24:4236–44.
  14. Thuerigen O, Schneeweiss A, Toedt G, et al. Gene expression signature predicting pathologic complete response with gemcitabine, epirubicin, and docetaxel in primary breast cancer. *J Clin Oncol* 2006;24:1839–45.
  15. Estevez LG, Gradishar WJ. Evidence-based use of neoadjuvant taxane in operable and inoperable breast cancer. *Clin Cancer Res* 2004;10:3249–61.
  16. Formenti SC, Symmans WF, Volm M, et al. Concurrent paclitaxel and radiation therapy for breast cancer. *Semin Radiat Oncol* 1999;9:34–42.
  17. Formenti SC, Volm M, Skinner KA, et al. Preoperative twice-weekly paclitaxel with concurrent radiation therapy followed by surgery and postoperative doxorubicin-based chemotherapy in locally advanced breast cancer: a phase I/II trial. *J Clin Oncol* 2003;21:864–70.
  18. Mason KA, Kishi K, Hunter N, et al. Effect of docetaxel on the therapeutic ratio of fractionated radiotherapy *in vivo*. *Clin Cancer Res* 1999;5:4191–8.
  19. Chakravarthy AB, Kelley MC, McLaren B, et al. Neoadjuvant concurrent paclitaxel and radiation in stage II/III breast cancer. *Clin Cancer Res* 2006;12:1570–6.
  20. Cornett DS, Mobley JA, Dias EC, et al. A novel histology-directed strategy for MALDI-MS tissue profiling that improves throughput and cellular specificity in human breast cancer. *Mol Cell Proteomics* 2006;5:1975–83.
  21. Barbieri CE, Perez CA, Johnson KN, Ely KA, Billheimer D, Pietenpol JA. IGFBP-3 is a direct target of transcriptional regulation by  $\Delta$ Np63 $\alpha$  in squamous epithelium. *Cancer Res* 2005;65:2314–20.
  22. Barbieri CE, Tang LJ, Brown KA, Pietenpol JA. Loss of p63 leads to increased cell migration and up-regulation of genes involved in invasion and metastasis. *Cancer Res* 2006;66:7589–97.
  23. Benjamini B, Hochberg Y. Controlling the false discovery rate: a practical and powerful approach to multiple testing. *J R Stat Soc Ser B* 1995;57:285–90.
  24. Neve RM, Chin K, Fridlyand J, et al. A collection of breast cancer cell lines for the study of functionally distinct cancer subtypes. *Cancer Cell* 2006;10:515–27.
  25. Debnath J, Brugge JS. Modelling glandular epithelial cancers in three-dimensional cultures. *Nat Rev Cancer* 2005;5:675–88.
  26. Kenny PA, Lee GY, Myers CA, et al. The morphologies of breast cancer cell lines in three-dimensional assays correlate with their profiles of gene expression. *Mol Oncol* 2007;1:84–96.
  27. Wang SE, Xiang B, Guix M, et al. Transforming growth factor  $\beta$  engages TACE and ErbB3 to activate phosphatidylinositol-3 kinase/Akt in ErbB2-overexpressing breast cancer and desensitizes cells to trastuzumab. *Mol Cell Biol* 2008;28:5605–20.
  28. Verhaegen M, Bauer JA, Martin de la Vega C, et al. A novel BH3 mimetic reveals a mitogen-activated protein kinase-dependent mechanism of melanoma cell death controlled by p53 and reactive oxygen species. *Cancer Res* 2006;66:11348–59.
  29. Albrethsen J, Bogebo R, Gammeltoft S, Olsen J, Winther B, Raskov H. Upregulated expression of human neutrophil peptides 1, 2 and 3 (HNP 1–3) in colon cancer serum and tumours: a biomarker study. *BMC Cancer* 2005;5:8.
  30. Roesch-Ely M, Nees M, Karsai S, et al. Proteomic analysis reveals successive aberrations in protein expression from healthy mucosa to invasive head and neck cancer. *Oncogene* 2007;26:54–64.
  31. Vlahou A, Schellhammer PF, Mendrinos S, et al. Development of a novel proteomic approach for the detection of transitional cell carcinoma of the bladder in urine. *Am J Pathol* 2001;158:1491–502.
  32. Ganz T. Defensins: antimicrobial peptides of innate immunity. *Nat Rev Immunol* 2003;3:710–20.
  33. Amann JM, Chaurand P, Gonzalez A, et al. Selective profiling of proteins in lung cancer cells from fine-needle aspirates by matrix-assisted laser desorption ionization time-of-flight mass spectrometry. *Clin Cancer Res* 2006;12:5142–50.
  34. Nishio K, Arioka H, Ishida T, et al. Enhanced interaction between tubulin and microtubule-associated protein 2 via inhibition of MAP kinase and CDC2 kinase by paclitaxel. *Int J Cancer* 1995;63:688–93.
  35. Blumcke I, Muller S, Buslei R, Riederer BM, Wiestler OD. Microtubule-associated protein-2 immunoreactivity: a useful tool in the differential diagnosis of low-grade neuroepithelial tumors. *Acta Neuropathol* 2004;108:89–96.
  36. Chen JY, Chang YL, Yu YC, et al. Specific induction of the high-molecular-weight microtubule-associated protein 2 (hmw-MAP2) by betel quid extract in cultured oral keratinocytes: clinical implications in betel quid-associated oral squamous cell carcinoma (OSCC). *Carcinogenesis* 2004;25:269–76.
  37. Liu Y, Mangini J, Saad R, et al. Diagnostic value of microtubule-associated protein-2 in Merkel cell carcinoma. *Appl Immunohistochem Mol Morphol* 2003;11:326–9.
  38. Liu Y, Sturgis CD, Grzybicki DM, et al. Microtubule-associated protein-2: a new sensitive and specific marker for pulmonary carcinoma tumor and small cell carcinoma. *Mod Pathol* 2001;14:880–5.
  39. Soltani MH, Pichardo R, Song Z, et al. Microtubule-associated protein 2, a marker of neuronal differentiation, induces mitotic defects, inhibits growth of melanoma cells, and predicts metastatic potential of cutaneous melanoma. *Am J Pathol* 2005;166:1841–50.
  40. Perou CM, Jeffrey SS, van de Rijn M, et al. Distinctive gene expression patterns in human mammary epithelial cells and breast cancers. *Proc Natl Acad Sci U S A* 1999;96:9212–7.
  41. Perou CM, Sorlie T, Eisen MB, et al. Molecular portraits of human breast tumours. *Nature* 2000;406:747–52.
  42. Sorlie T, Perou CM, Tibshirani R, et al. Gene expression patterns of breast carcinomas distinguish tumor subclasses with clinical implications. *Proc Natl Acad Sci U S A* 2001;98:10869–74.
  43. Sorlie T, Tibshirani R, Parker J, et al. Repeated observation of breast tumor subtypes in independent gene expression data sets. *Proc Natl Acad Sci U S A* 2003;100:8418–23.
  44. Kreike B, van Kouwenhove M, Horlings H, Weigelt B, Bartelink H, Van de Vijver MJ. Gene expression profiling and histopathological characterization of triple negative/basal-like breast carcinomas. *Breast Cancer Res* 2007;9:R65.
  45. Carey LA, Dees EC, Sawyer L, et al. The triple negative paradox: primary tumor chemosensitivity of breast cancer subtypes. *Clin Cancer Res* 2007;13:2329–34.
  46. Rouzier R, Perou CM, Symmans WF, et al. Breast cancer molecular subtypes respond differently to preoperative chemotherapy. *Clin Cancer Res* 2005;11:5678–85.
  47. Chen H, Xu Z, Peng L, et al. Recent advances in the research and development of human defensins. *Peptides* 2006;27:931–40.
  48. Dehmelt L, Halpain S. The MAP2/Tau family of microtubule-associated proteins. *Genome Biol* 2005;6:204.
  49. Veitia R, David S, Barbier P, et al. Proteolysis of microtubule associated protein 2 and sensitivity of pancreatic tumours to docetaxel. *Br J Cancer* 2000;83:544–9.
  50. Henderson IC, Berry DA, Demetri GD, et al. Improved outcomes from adding sequential paclitaxel but not from escalating doxorubicin dose in an adjuvant chemotherapy regimen for patients with node-positive primary breast cancer. *J Clin Oncol* 2003;21:976–83.